



AIAS 2018 International Conference on Stress Analysis

## Design and manufacture of hybrid aluminum/composite co-cured tubes with viscoelastic interface layer

Marco Povolo<sup>a\*</sup>, Luca Raimondi<sup>b</sup>, Tommaso Maria Brugo<sup>a</sup>, Angelo Pagani<sup>c</sup>, Dario Comand<sup>c</sup>, Luca Pirazzini<sup>c</sup>, Andrea Zucchelli<sup>a,b\*</sup>

<sup>a</sup>DIN – Università di Bologna, Viale Risorgimento 2, 40136 Bologna, Italia

<sup>b</sup>CIRI-MAM – Università di Bologna, Viale Risorgimento 2, 40136 Bologna, Italia

<sup>c</sup>REGLASS SRL – Via Caduti di Cefalonia, 4, 40061 Minerbio BO, Italia

### Abstract

The development of hybrid FRP-metal axisymmetric components is a matter of increasing interest in the automotive and aerospace industry for a lightweight design. The hybridization of the technology enables a cost reduction of components production and an increase of mechanical performances together with the ability of machining the surface of the metal tube; this technique guarantees a production improvement since the coating of the tube is no longer required and the pieces can be manufactured in one-step curing cycle. The improvement in bending and torsional stiffness, corrosion resistance and mass reduction of hybrid tubes, in comparison to the single material-built component, has been already demonstrated. A great challenge is to find a way to make hybrid tubes with external metal, avoiding delaminations and detachments that could occur during and after the curing process, due to the different coefficients of thermal expansion between FRP and metal along the axial direction of the tube. For this reason, a component manufacturing process has been studied by experimental and numerical analysis (FEM), including custom process machines and inserting a viscoelastic layer as an interface between the two tubes. Genetic algorithm method has been used to optimize the stacking sequence of a hybrid co-cured metal/composite tube to maximize the flexural stiffness, while applying a strength constraint condition.

© 2018 The Authors. Published by Elsevier B.V.

This is an open access article under the CC BY-NC-ND license (<http://creativecommons.org/licenses/by-nc-nd/3.0/>)

Peer-review under responsibility of the Scientific Committee of AIAS 2018 International Conference on Stress Analysis.

*Keywords:* Composite; Cylinder; Optimization; Bending; Hybrid Tubes; CFRP;

\* Corresponding author. Tel.: +39 051 209 3457

E-mail address: [a.zucchelli@unibo.it](mailto:a.zucchelli@unibo.it)

E-mail address: [marco.povolo2@unibo.it](mailto:marco.povolo2@unibo.it)

## 1. Introduction

The increased performances of hybrid pipes and tubular section geometries are desirable in several industry for their higher natural frequencies and bearing stress capability with respect to their metal counterpart. In some industrial applications, the possibility to have a metal coating on the external part of the pipe is desirable for their antistatic properties, improved corrosion resistance and improved tribological properties. Moreover, metal coatings offer the possibility to perform thermal spray treatments for a functionalization of the surface.

Hybrid tubular components has been successfully manufactured in several ways, each one with their specific limitation. Adhesive bonding is commonplace but is applicable only for small components and requires a two-step manufacturing process (Jeon et al. (2016); Wang et al. (2016)). Interference coupling is usually obtained by heating or cooling the metal part, but the process tends to perform slow in production and requires again two steps cycles.

Co-curing is a novel promising technology that enables the production of a hybrid tube in one step manufacturing process, able to provide cost and time savings. However, despite their attractive advantages, the manufacturing tasks associated with hybrid metal/composite co-cured tubes are still a challenge in their design process and few and recent studies has been published on the topic.

The manufacturing process of co-cured, hybrid, aluminum-core shaft, was studied by Cho et al. (1998). Their investigation showed that the quality of the component is strictly connected with the axial residual thermal stresses due to the large difference of coefficient of thermal expansion (CTE) of the two materials. To reduce the residual thermal stresses, the use of a compressive preload by the employment of a steel jig was suggested.

A similar solution for the design and manufacturing of a co-cured hybrid aluminum drive shaft was suggested by Lee et al. (2004). The effects of thermal stresses were again reduced by inducing a compressive preload on metal tube and the stacking sequence was selected by minimizing the failure index according to Tsai Wu criterion. An interface made of glass fiber epoxy composite was introduced to reduce galvanic corrosion between the aluminum and the carbon fiber composite, but authors found a higher failure index.

Han et al. (2017) found a solution for design and manufacturing of a conical co-cured hybrid pantograph upper arm using a frictional layer to avoid the excessive stress and possible failure in the bonding layers between the composite laminate and aluminum tube. The hybrid structure was designed to reduce the mass and to enhance the structural stiffness. At least, they design a metal-composite hybrid metal arm that exhibit a much higher mechanical performance than a conventional steel arm avoiding material failure.

So far, from the state of the art analysis, it is clear that a key aspect in design and manufacturing of hybrid tubes is the reduction of the residual stress peak to avoid premature failure of the component; the adopted strategies to reach this task are based on the variation of the stacking sequence and by changing the materials at the interface between metal and composite.

To the best author knowledge, this is the first study on hybrid co-cured metal composite tube that employs a viscoelastic interface layer and an optimization of the stacking sequence based on numeric algorithm to minimize the possibility of premature failure and maximize the flexural stiffness. Additionally, an experimental procedure for validating FEA result is proposed. Moreover, due to the viscoelastic properties of the interface, jig is no longer required and tubes can be made in one-step manufacturing cycle.

### Nomenclature

|             |      |                                    |
|-------------|------|------------------------------------|
| $D_{iCFRP}$ | [mm] | internal diameter of CFRP tube     |
| $D_{eCFRP}$ | [mm] | external diameter of CFRP tube     |
| $D_{iAL}$   | [mm] | internal diameter of aluminum tube |
| $D_{eAL}$   | [mm] | external diameter of aluminum tube |
| $l$         | [mm] | length of tube                     |
| $S_{CFRP}$  | [mm] | CFRP thickness                     |
| $S_{AL}$    | [mm] | aluminum thickness                 |

|                      |                      |  |
|----------------------|----------------------|--|
| $s_i$                | [mm]                 | interface layer thickness                        |
| $E$                  | [MPa]                | elastic modulus                                  |
| $E_L$                | [MPa]                | longitudinal elastic modulus                     |
| $E_T$                | [MPa]                | transverse elastic modulus                       |
| $G$                  | [MPa]                | shear modulus                                    |
| $G_{LT}$             | [MPa]                | orthotropic shear modulus                        |
| $\nu_{LT}$           |                      | orthotropic Poisson's ratio                      |
| $\rho$               | [Kg/m <sup>3</sup> ] | density  |
| $\alpha$             | [1/°C]               | coefficient of thermal expansion                 |
| $\alpha_L$           | [1/°C]               | longitudinal coefficient of thermal expansion    |
| $\alpha_T$           | [1/°C]               | transverse coefficient of thermal expansion      |
| $\sigma_{ut}$        | [MPa]                | tensile strength                                 |
| $\sigma_{L,rupture}$ | [MPa]                | orthotropic stress limit, traction $l$ direction |
| $\sigma_{T,rupture}$ | [MPa]                | orthotropic stress limit, traction $t$ direction |
| $\tau_{LT,rupture}$  | [MPa]                | orthotropic stress limit, shear $lt$             |

**2. Materials and Methods**

The procedure adopted in the present work combines numerical analysis and experimental tests in order to set-up the design procedure of a hybrid tube with a low impact of residual stresses and minimum deflection under constant bending moment. This loading condition and the well-defined geometry are specific for the field of application of industrial printing machines.

*2.1. Design and materials*

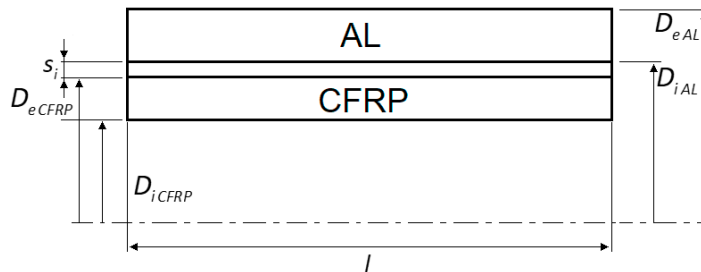


Fig.1. Geometric scheme

The total length of the test tube was 900 mm and the external diameter of the metal tube was 75 mm. The design thickness of the composite was 2.2 mm as a compromise with stiffness and functional requirement. The design thickness of the extruded aluminum tube, made in 6082-T6 alloy, was 2.5 mm.

Mechanical properties of UD, viscoelastic interface layer, epoxy resin and aluminum alloy are provided in table 2, 3, 4 and 5 respectively. The stacking sequence initially consisted of 6 layers of unidirectional (UD) CFRP prepreg in the axial direction, which is fundamental for guaranteeing performance and for validating the FEA results. The

prepreg named M23350R was supplied by Reglass Srl, Minerbio (BO) Italy. This material is manufactured using Toray T300 and impregnated with a 55% in volume (Vf) of custom epoxy resin EP200 supplied by Reglass Srl, also used as an interface layer in FEA interlayers comparison. The prepreg was laminated in a clean room at 24 °C and the curing temperature was 110° C.

Table 1. Geometric properties of the tube

| Properties | $D_{iCFRP}$ | $D_{eCFRP}$ | $D_{iAL}$ | $D_{eAL}$ | $l$  | $S_{CFRP}$ | $S_{AL}$ | $S_i$ |
|------------|-------------|-------------|-----------|-----------|------|------------|----------|-------|
|            | (mm)        | (mm)        | (mm)      | (mm)      | (mm) | (mm)       | (mm)     | (mm)  |
| Value      | 64.6        | 69.0        | 70.0      | 75.0      | 900  | 2.2        | 2.5      | 0.5   |

Table 2. Prepreg properties, M23350R (Reglass Srl)

| Properties | $E_L$  | $E_T$ | $G_{LT}$ | $\nu_{LT}$ | $\rho$               | $\alpha_L$               | $\alpha_T$           | $\sigma_{L,rupture}$ | $\sigma_{T,rupture}$ | $\tau_{LT,rupture}$ |
|------------|--------|-------|----------|------------|----------------------|--------------------------|----------------------|----------------------|----------------------|---------------------|
|            | (MPa)  | (MPa) | (MPa)    |            | (Kg/m <sup>3</sup> ) | (1/°C)                   | (1/°C)               | (MPa)                | (MPa)                | (MPa)               |
| Value      | 115100 | 7700  | 4400     | 0.33       | 1630                 | -2.7<br>10 <sup>-7</sup> | 4.1 10 <sup>-5</sup> | 2200                 | 30                   | 60                  |

Table 3. Interface viscoelastic layer (Reglass)

| Properties | $E^*$ | $G^*$ | $\rho$               | $\sigma_{ut}$ | $E_{50\%}$ |
|------------|-------|-------|----------------------|---------------|------------|
|            | (MPa) | (MPa) | (Kg/m <sup>3</sup> ) | (MPa)         | (MPa)      |
| Value      | 270   | 90    | 1250                 | 15.0          | 12.5       |

\*according to DIN 53504 calculated data (at 1% elongation).

Table 4. Epoxy resin EP200 (Reglass)

| Properties | $E$   | $G$   | $\rho$               | $\sigma_{ut}$ | $\alpha$             |
|------------|-------|-------|----------------------|---------------|----------------------|
|            | (MPa) | (MPa) | (Kg/m <sup>3</sup> ) | (MPa)         | (1/°C)               |
| Value      | 2000  | 1600  | 1100                 | 130.0         | 6.0 10 <sup>-5</sup> |

Table 5. Aluminum tube (6082-T6) properties

| Properties | $E$   | $\rho$               | $\alpha$             |
|------------|-------|----------------------|----------------------|
|            | (MPa) | (Kg/m <sup>3</sup> ) | (1/°C)               |
| Value      | 70000 | 2700                 | 2.4 10 <sup>-5</sup> |

## 2.2. Manufacturing process

An innovative process has been implemented to produce hybrid tubes according to the process depicted in Fig 2.

- 1) First, a cylindrical mandrel with silicon body was prepared and cleaned with methylethylketone.
- 2) Prepreg layers were stacked with a suitable overlap on the surface.
- 3) A mandrel was inserted into the external metal tube and metal bushings were inserted to maintain the axial symmetry of the component.
- 4) Pressure of 3 bar was then given to expand the silicon surface of the mandrel and the prepreg and viscoelastic layer were forced to adhere to the inner area of the metal cylinder. In this condition the curing phase of the entire component was able to take place.
- 5) Once the curing cycle is over, the pressure was raised, and the mold was extracted
- 6) The component was machined finished.

This manufacturing process uses the low elastic modulus of the interface layer to compensate the deformations due to the different CTE during the cooling phase. This allow to avoid the usage of a jig as suggested by Cho et al. (1998) and Kim et al. (2004).

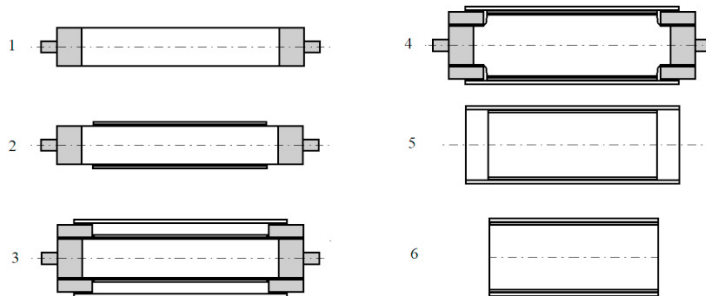


Fig. 2. Production process scheme

The proposed manufacturing process was successfully used to prepare a first batch of hybrid co-cured tube with the geometrical properties depicted in Tab. 1 and with a stacking sequence of  $[0^\circ]_6$  along the axial direction. In Fig. 3 a micrograph of the so manufactured tube is shown and no delamination phenomena were detected.

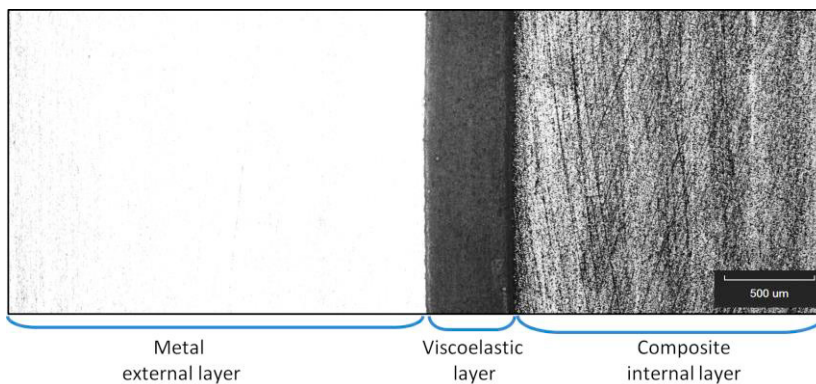


Fig. 3. Production process scheme

### 3. Finite Element Model and experimental validation

#### 3.1. FEM model and stress analysis

In order to better understand the distribution of the residual stresses at the free edges, finite element analysis (FEA) has been performed. The symmetry of both geometry and loads allowed to study a quarter of cylinder in order to reduce computation time. The FEA model was thermally loaded and the cooling phase was simulated adopting an implicit solver. The tube was modeled in Ansys using SOLID186 elements. SOLID186 is a higher order 3-D 20-node solid element that exhibits quadratic displacement behavior. Reduced integration was used to minimize locking phenomena without using the layered option. The composite was therefore modeled using a layer by layer configuration in order to better describe the shear phenomena. The viscoelastic layer (Table 3) was modeled selecting a bilinear material behavior (Young's modulus 220 MPa, Yield strength 7 MPa, Tangent Modulus 10 MPa) in a simple static structural thermal analysis as approximation of the cooling cycle. A mesh convergence test was conducted to minimize the stress error and to respect the zero stress conditions at the free edges. The mesh was refined at free edge and it was found that the maximum element size to correctly represent the stress distributions is 0.01 mm in axial direction.

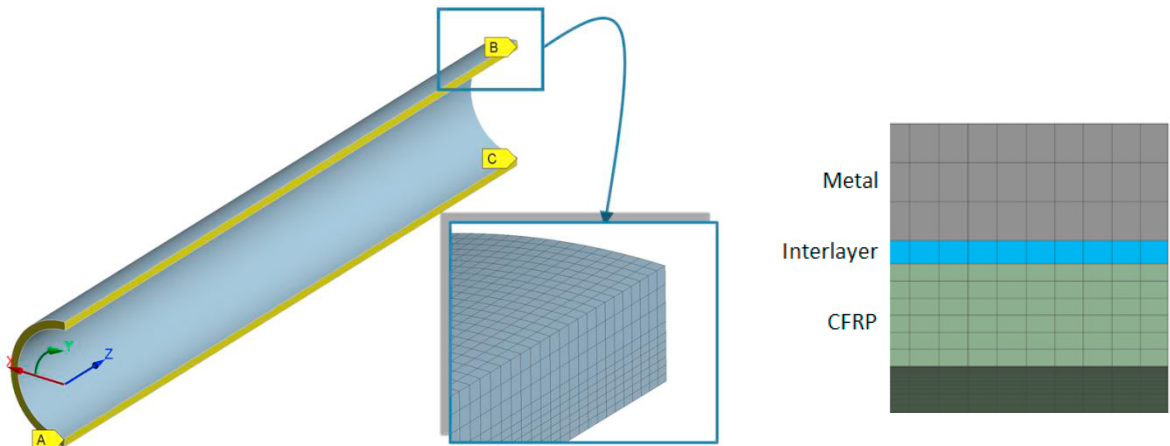


Fig. 4 Meshed tube and constrain

Contact elements were not introduced to reduce the computational time without reducing precision. The model so build and constrained is represented in Fig. 4. Face marked with letter A was constrained in axial (z) direction and both faces B and C were constrained in circumferential direction (y). Thanks to the model it was possible to investigate the influence of the interface layer material on stress and strain distribution along the axial direction. It was found that the most critical stress is the shear stress  $\tau_{rz}$  developed between the aluminum and the composite. A comparison of the shear stress distribution at the centerline of the adhesive interlayer is represented in Fig.5, for both epoxy EP200 (blue curve) and viscoelastic interlayer (red curve). For the case of the epoxy EP200 interlayer, material stress concentration occurs approximately at 0.7 mm from the free edge, with a maximum absolute value of 30 MPa. This value is above the critical shear strength of commonly used epoxy adhesives and therefore makes this solution not feasible. On the contrary, for the viscoelastic layer, the curve shows a large “plateau” close to the free edge zone, due to the elastoplastic behavior of the material. For this reason, the viscoelastic interface layer was chosen for the construction of the tubes.

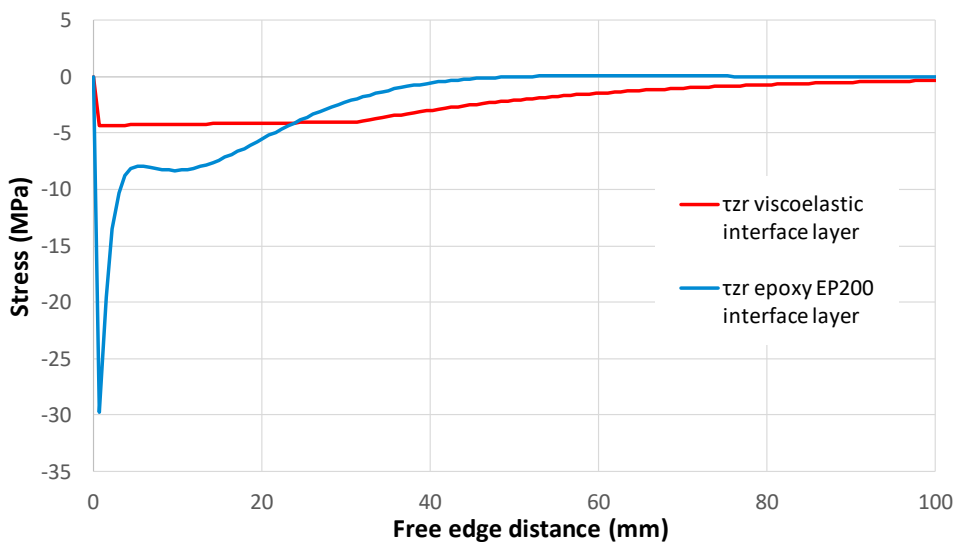


Fig.5. FEM Shear stresses comparison between two materials in the interface layer at the end of the tube.

### 3.2. Experimental validation

Test tubes was manufactured with all 6 layers at  $0^\circ$  in the axial direction to validate the stress analysis calculated using FEM using the viscoelastic material as interface layer according to Fig.5 results. Subsequently, 2 self-temperature-compensated strain gauges were applied at the center of tube to monitor axial and hoop strain evolution during the whole curing cycle. It was found that the after curing axial and hoop strain differs from the numerical model of less than 7% and 4%, respectively. This small error ensures a good accuracy in the optimization procedure.



Fig. 6. Experimental set-up

## 4. Optimization and results

In common practice, the optimization process of a composite structure is dominated by one or more objective functions, design variables and constraints (Nikbakt (2018)). In the present work, a failure index of 0.7 according to Hashin 3D criteria as been assumed as a constrain. Hashin 3D is an interactive failure criteria that enables to detect fiber or matrix failure and is able to describe as well the interlaminar one (Cesari (2007)). The minimization of the deflection under pure bending load has been set as objective function. The stacking sequence angles of the 6 layers that composes the laminate were set as a continuous variable. The optimization was performed using the “surrogate model” proposed in the Design Of Experiment (DOE) module of Ansys, in order to evaluate the influence of the variables on the responses and reducing the global computational time. After the DOE was performed, the tube has been optimized by a Multi-Objective Genetic Algorithm (MOGA). The best solution obtained with MOGA foresees a predominance of layers at almost zero degrees, with the exception of the first two in contact with the viscoelastic layer (Table 5). This solution provided a failure index of 0.68, but manufacturability limits imposes to use discrete angles for the prepreg wrapping sequence. For this reason, a new simulation with manufacturable layers angles (Table 5) was carried out and the result were compared. An acceptable 3% increase of the deflection was obtained with a failure index of 0.63

Table 6. Stacking sequence comparison

| Layer number | Optimization angle value (°) | Equivalent manufacturing angle value (°) |
|--------------|------------------------------|--|
| 1            | -19.8                        | -30                                      |
| 2            | +42.6                        | +30                                      |
| 3            | -5.4                         | 0  |
| 4            | -0.9                         | 0  |
| 5            | -3.7                         | 0  |
| 6            | -9.2                         | 0  |

## 5. Conclusion

In this study a manufacturing process, an experimental validation and an optimization of the stacking sequence for hybrid co-cured aluminum/composite tube with interface layer under constant bending moment is proposed.

In particular, for the first time a one-step, cost effective, manufacturing process of a hybrid metal-composite tube is proposed. The process was successfully implemented and used to realize a first batch of hybrid-metal composite tubes. Micrograph analysis reveal no defect in the composite and perfect bonding between the viscoelastic layer and both metal and composites layers, thus demonstrating the effectiveness of the new process. Moreover, the results of the experimental analysis together with the numerical simulations of the hybrid tubes, gave the conclusion that:

- the numerical model well represented the real behavior of the hybrid tube;
- the viscoelastic interface layer between aluminum and CFRP tube, compared to the configuration with an epoxy interface layer, is effective to reduce thermal residual stress peaks thus providing a suitable failure index for the entire part.

Thanks to the preliminary setup of the numerical model it was possible to establish a robust procedure for the optimization of the composite stacking sequence. Manufacturability was ensured by perform a further simulation with discrete ply angles close to the optimal solution.

In this work, only laminate with a constant thickness and composite tube with defined number of layers and defined geometry was analyzed. In the future, different type of stacking sequence and geometry constraints will also be investigated.

## Acknowledgments

This work was funded by Emilia Romagna region (Italy), POR-FESR ER, Research and innovation – Priority axis 1. Sviluppo di una tecnologia innovativa per la produzione di nuovi rulli ibridi metallo-carbonio CUP E88C15000320007

## References

- Cesari, F., Dal Re, V., Minak, G., & Zucchelli, A., 2007. Damage and residual strength of laminated carbon–epoxy composite circular plates loaded at the centre. *Composites Part A: Applied Science and Manufacturing*, 38(4), 1163-1173.
- Cho, D. H., & Lee, D. G., 1998. Manufacturing of co-cured composite aluminum shafts with compression during co-curing operation to reduce residual thermal stresses. *Journal of composite materials*, 32(12), 1221-1241.
- Han, M. G., Cho, Y. H., Jeon, S. W., & Chang, S. H., 2017. Design and fabrication of a metal-composite hybrid pantograph upper arm by co-cure technique with a friction layer. *Composite Structures*, 174, 166-175.
- Jeon, S. W., Cho, Y. H., Han, M. G., & Chang, S. H., 2016. Design of carbon/epoxy–aluminum hybrid upper arm of the pantograph of high-speed trains using adhesive bonding technique. *Composite Structures*, 152, 538-545.
- Kim, H. S., Kim, J. W., & Kim, J. K., 2004. Design and manufacture of an automotive hybrid aluminum/composite drive shaft. *Composite structures*, 63(1), 87-99.
- Nikbakt, S., Kamarian, S., & Shakeri, M., 2018. A Review on Optimization of Composite Structures Part I: Laminated Composites. *Composite Structures*.
- Wang, J., Gao, H., Ding, L., Hao, Y., Wang, B., Sun, T., & Liang, Y., 2016. Bond strength between carbon fiber–reinforced plastic tubes and aluminum joints for racing car suspension. *Advances in Mechanical Engineering*, 8(10), 1687814016674627.